Angewandte Chemie
Eine Zeitschrift der Gesellschaft Deutscher Chemiker

Supporting Information

© Wiley-VCH 2007

69451 Weinheim, Germany

Supporting Information

On the Biradicaloid Nature of Long Quinoidal Oligothiophenes: New Experimental Evidences Guided by Theoretical Studies.

Rocío Ponce Ortiz, Juan Casado, Víctor Hernández, Juan T. López Navarrete, Pedro M. Viruela, Enrique Ortí,* Kazuo Takimiya, Tetsuo Otsubo*

R. Ponce, Dr. J. Casado, Prof. V. Hernández, Prof. J. T. López Navarrete

Departamento de Química Física, Universidad de Málaga, 29071 Málaga (Spain)

Fax: (+34)952132000

E-mail: teodomiro@uma.es

Prof. P. M. Viruela, Prof. E. Ortí

Institut de Ciència Molecular, Universitat de València, 46980 Paterna (Spain)

Fax: (+34)963543274

E-mail: enrique.orti@uv.es

Dr. Kazuo Takimiya, Prof. Tetsuo Otsubo

Department of Applied Chemistry, Graduate School of Engineering, Hiroshima University, Higashi-Hiroshima 739-8527, Japan

1. Theoretical Calculations and Experimental Details

All theoretical calculations were carried out using the Gaussian 03 program package.[1] Calculations to investigate the molecular and electronic structures of quinoidal oligothiophenes Q*n* (*n* = 1−6) were mainly performed within the density functional theory (DFT) approach using the Becke's three-parameter B3LYP exchange-correlation functional[2] and the 6-31G** basis set.[3] The chemical structure of Q*n* was simplified by substituting the pendant butoxymethyl groups by metoxymethyl groups. This structural change is not expected to affect the electronic properties and reduces considerably the number of atoms (from 286 to 178 for Q6) and the size of the basis set (from 2754 to 1854 atomic orbitals for Q6). The geometries of Q*n* were fully optimized within C_{2v} (odd oligomers) and C_{2h} (even oligomers) symmetry restrictions. Release of the symmetry constraints did not change the geometries and the molecules remain mainly planar, as was tested for the trimer Q3.

Q*n* compounds were first calculated as closed-shell (CS) singlets at the spin-restricted RB3LYP/6-31G** level. This approach yields well-defined quinoidal geometries for Q1 to Q6 with short C_α-$C_{\alpha'}$ and C_β-$C_{\beta'}$ bonds and long C_α-C_β bonds (see Figures S2 to S4). The stability of the RB3LYP/6-31G** wave function was checked and it was found to become unstable (RHF to UHF instability)[4] for Q4, Q5 and Q6. Q*n* compounds were then reoptimized as open-shell (OS) singlets using an spin-unrestricted broken-symmetry (BS) UB3LYP(BS)/6-31G** function. This approach uses the Guess = mix keyword to build up, as the initial guess wave function, a 1:1 mixture of the singlet and triplet states, with a spin-squared expectation value $\langle S^2 \rangle = 1$,[5] and has been shown to provide reliable geometries and energies for singlet-state biradicals.[6] Davidson and Clark recently concluded that BS-UDFT is the most consistent choice for studying large systems with biradical character where high-level ab initio calculations are not feasible.[6c] UB3LYP(BS) calculations converge to the

R3B3LYP solutions for Q1, Q2 and Q3, showing that the ground state of these oligomers is well-described as a closed-shell singlet. For Q4, Q5 and Q6, the UB3LYP(BS) solution is lower in energy than the RB3LYP solution and the ground state of these oligomers is best described as an open-shell singlet with a partial biradical character that grows up with the oligomer length. To support the DFT results, CASSCF calculations using an active space limited to two electrons in the two frontier molecular orbitals HOMO and LUMO were performed. CASSCF(2,2)/6-31G calculations were carried out on the UB3LYP(BS)/6-31G** optimized geometries for Q4, Q5 and Q6. Q*n* compounds were finally optimized as triplets at the UB3LYP/6-31G** level (see Figures S2, S3 and S4).

Vertical electronic excitations energies were computed using the time-dependent DFT (TD-DFT) approach.[7] This approach provides excitation energies in good agreement with the experiment for the low-lying valence excited states of most closed-shell compounds,[8] and has been successfully applied for singlet biradical compounds.[9] $S_0 \rightarrow S_n$ excitation energies were calculated at both the RB3LYP/6-31G** and the UB3LYP(BS)/6-31G** levels using the geometries optimized for S_0 at the respective theory levels. $T_1 \rightarrow T_n$ excitation energies were obtained at the UB3LYP/6-31G** level using the optimized geometry of T_1.

Figure S1 shows the atomic orbital composition calculated for the frontier molecular orbitals of aromatic T3 and quinoid Q3 at the RB3LYP/6-31G** level. Table S1 lists the total energies calculated for Q1 to Q6 as closed-shell singlets (RB3LYP/6-31G**), open-shell singlets (UB3LYP(BS)/6-31G**) and triplets (UB3LYP/6-31G**). Figures S2, S3 and S4 collect the values of selected bond lengths optimized for Q3, Q4, Q5 and Q6 in the singlet ground state S_0 and in the triplet state T_1. Table S2 summarizes the C=C/C–C bond length alternation (BLA) values calculated for Q2 to Q6. The BLA parameter is calculated for each thiophene ring as the difference between the length of the C_β-$C_{\beta'}$ bond and the average of the

C_α-C_β and $C_{\alpha'}$-$C_{\beta'}$ bonds. A quinoidal ring is thus characterized by a negative BLA value, while an aromatic ring shows a positive BLA value. The BLA parameter thus illustrates how the quinoid/aromatic character of the molecule varies with the length of the oligomer and with the electronic state. Figure S5 shows the atomic spin densities calculated for the T_1 state of Q6 at the UB3LYP/6-31G** level

FT-Raman scattering spectra were collected on a Bruker FRA106/S apparatus and a Nd:YAG laser source (λ_{exc} = 1064 nm), in a back-scattering configuration. The operating power for the exciting laser radiation was kept to 100 mW in all the experiments. Samples were analyzed as pure solids averaging 1000 scans with 2 cm^{-1} of spectral resolution.
Resonance Raman spectra (λ_{exc} = 514 nm) were recorded by using a Microscope Invia Reflex Raman RENISHAW.

A variable temperature cell (Specac P/N 21526) with interchangeable pairs of quartz windows was used to record the FT-Raman spectra at different temperatures. This is equipped with a Cu- constantan thermocouple for temperature-monitoring purposes, and any temperature from –170 to +150 °C can be achieved. Spectra were recorded after waiting for thermal equilibrium at the sample, which required 20 min for every increment of 10 °C.

Table S1: Total energies (in a.u.) calculated at the B3LYP/6-31G** level for the singlet ground state S_0 (closed-shell (CS) and open-shell (OS)) and for the triplet state T_1 of compounds Q1 to Q6.

Compound	S_0 (CS)[a]	S_0 (OS)[b]	T_1[c]
Q1	–1423.763608	–1423.763608	–1423.720186
Q2	–2399.992326	–2399.992326	–2399.965276
Q3	–3376.214637	–3376.214637	–3376.198896
Q4	–4352.435261	–4352.435916	–4352.427836
Q5	–5328.655450	–5328.658685	–5328.654543
Q6	–6304.874835	–6304.881370	–6304.879222

[a]RB3LYP/6-31G** energies. [b]UB3LYP(BS)/6-31G** energies. [c]UB3LYP/6-31G** energies.

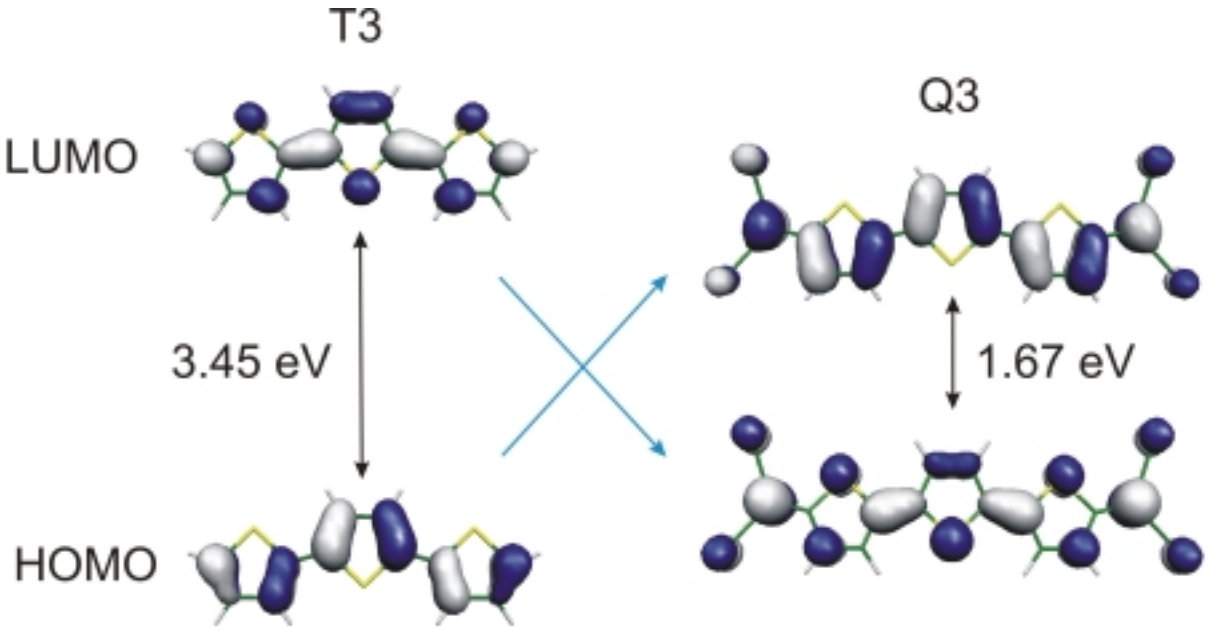

Figure S1. Electron density contours (0.03 e bohr^{-3}) calculated for the frontier molecular orbitals of aromatic terthiophene (T3) and quinoidal terthiophene (Q3) at the RB3LYP/6-31G** level. The bis(butoxymethyl)cyclopentane rings in Q3 show no contribution and have been omitted for simplicity.

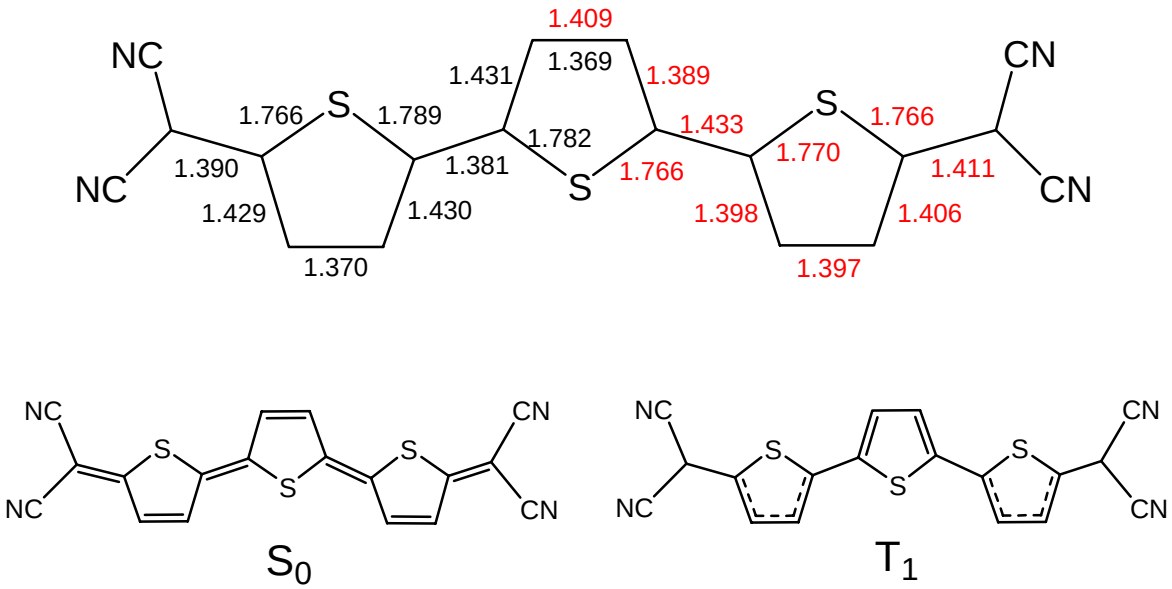

Figure S2. B3LYP/6-31G** optimized bond lengths (in Å) for Q3 (C_{2v} symmetry). Values in black refer to the closed-shell RB3LYP geometry of the singlet ground state S_0. Values in red refer to the open-shell UB3LYP geometry of the triplet state T_1. Schematic structures are drawn for S_0 and T_1 by considering bond distances below 1.390 Å as double bonds and those above 1.410 Å as single bonds. The bis(butoxymethyl)cyclopentane rings preserve the same geometry for both states (differences smaller than 0.002 Å) and have been omitted for simplicity.

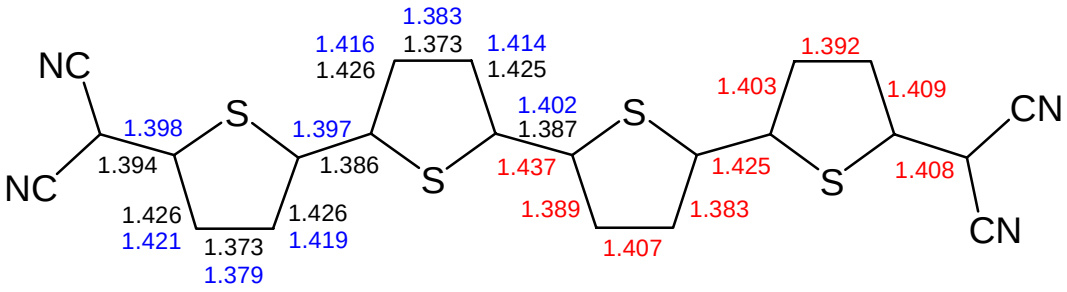

Figure S3. B3LYP/6-31G** optimized bond lengths (in Å) for Q4 (C_{2h}). Values in black refer to the closed-shell RB3LYP geometry of the singlet ground state S_0. Values in blue refer to the open-shell UB3LYP(BS) geometry of the singlet ground state state S_0. Values in red refer to the open-shell UB3LYP geometry of the triplet state T_1. The bis(butoxymethyl)cyclopentane rings preserve the same geometry for both states and have been omitted for simplicity.

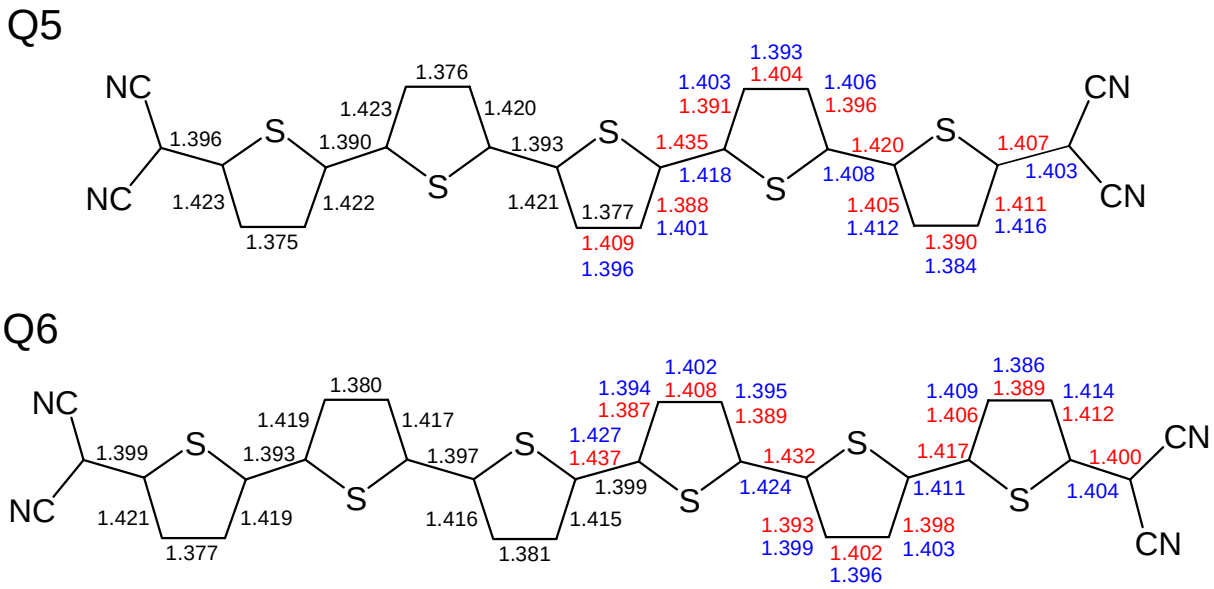

Figure S4. B3LYP/6-31G** optimized bond lengths (in Å) for Q5 (C_{2v}) and Q6 (C_{2h}). Values in black refer to the closed-shell RB3LYP geometry of the singlet ground state S_0. Values in blue refer to the open-shell UB3LYP(BS) geometry of the singlet ground state state S_0. Values in red refer to the open-shell UB3LYP geometry of the triplet state T_1. The bis(butoxymethyl)cyclopentane rings preserve the same geometry for both states and have been omitted for simplicity.

Table S2: C=C/C–C bond length alternation (BLA) values (in Å) calculated at the B3LYP/6-31G** level for the singlet ground state S_0 (closed-shell (CS) and open-shell (OS)) and for the triplet state T_1 of compounds Q2 to Q6.

Compound[a]		S_0 (CS)[b]	S_0 (OS)[c]	T_1[d]
Q2		–0.070		+0.011
Q3	ring 1	–0.062		+0.020
	ring 2	–0.060		–0.005
Q4	ring 1	–0.053	–0.032	+0.021
	ring 2	–0.053	–0.041	–0.014
Q5	ring 1	–0.044	–0.005	+0.021
	ring 2	–0.046	–0.012	+0.011
	ring 3	–0.048	–0.030	–0.018
Q6	ring 1	–0.035	+0.008	+0.020
	ring 2	–0.038	–0.005	+0.006
	ring 3	–0.043	–0.026	–0.020

[a]Thiophene rings are numbered starting from the center of the oligomer. [b]RB3LYP/6-31G**. [c]UB3LYP(BS)/6-31G**, the optimization converges to the RB3LYP/6-31G** geometry for Q2 and Q3. [d]UB3LYP/6-31G**.

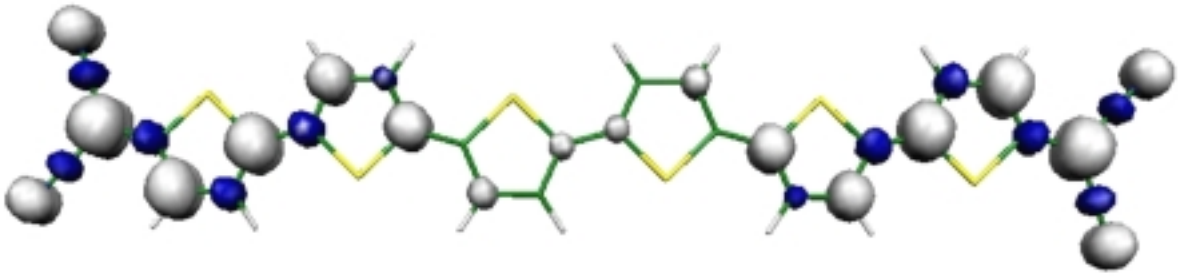

Figure S5. Spin density calculated at the UB3LYP/6-31G** level for the triplet state T_1 of Q6. Light and dark surfaces represent positive and negative spin densities, respectively. Bis(butoxymethyl)-cyclopentane moieties are omitted because they show no contribution.

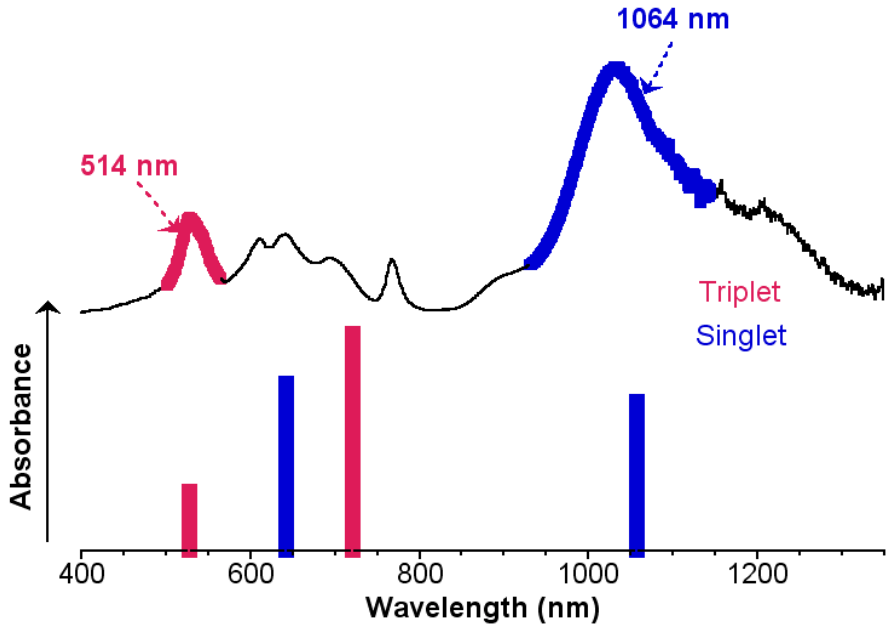

Figure S6. UV-Vis-NIR absorption spectrum of Q6. The wavelength ranges used for laser excitation in Resonance Raman spectra are marked in blue and red. Theoretical TDDFT electronic transitions predicted for Q6 in the most stable S_0 state (blue) and in the T_1 state (red) are indicated as vertical bars. For simplicity, excitations calculated with oscillator strengths lower than 0.4 have been omitted.

[1] Gaussian 03, Revision C.02, M. J. Frisch, G. W. Trucks, H. B. Schlegel, G. E. Scuseria, M. A. Robb, J. R. Cheeseman, Jr., J. A. Montgomery, T. Vreven, K. N. Kudin, J. C. Burant, J. M. Millam, S. S. Iyengar, J. Tomasi, V. Barone, B. Mennucci, M. Cossi, G. Scalmani, G. Rega, G. A. Petersson, H. Nakatsuji, M. Hada, M. Ehara, K. Toyota, R. Fukuda, J. Hasegawa, M. Ishida, T. Nakajima, Y. Honda, O. Kitao, H. Nakai, M. Klene, X. Li, J. E. Knox, H. P. Hratchian, J. B. Cross, V. Bakken, C. Adamo, J. Jaramillo, R. Gomperts, R. E. Stratmann, O. Yazyev, A. J. Austin, R. Cammi, C. Pomelli, J. W. Ochterski, P. Y. Ayala, K. Morokuma, G. A. Voth, P. Salvador, J. J. Dannenberg, V. G. Zakrzewski, S. Dapprich, A. D. Daniels, M. C. Strain, O. Farkas, D. K. Malick, A. D. Rabuck, K. Raghavachari, J. B. Foresman, J. V. Ortiz, Q. Cui, A. G. Baboul, S. Clifford, J. Cioslowski, B. B. Stefanov, G. Liu, A. Liashenko, P. Piskorz, I. Komaromi, R. L. Martin, D. J. Fox, T. Keith, M. A. Al-Laham, C. Y. Peng, A. Nanayakkara, M. Challacombe, P. M. W. Gill, B. Johnson, W. Chen, M. W. Wong, C. Gonzalez, J. A. Pople, Gaussian, Inc., Wallingford CT, 2004.

[2] A. D. Becke, *J. Chem. Phys.* **1993**, *98*, 1372–1377.

[3] M. M. Francl, W. J. Pietro, W. J. Hehre, J. S. Binkley, M. S. Gordon, D. J. Defrees, J. A. Pople, *J. Chem. Phys.* **1982**, *77*, 3654–3665.

[4] S. D. Kahn, W. J. Hehre, J. A. Pople, *J. Am. Chem. Soc*. **1987**, *109*, 1871–1873.

[5] Open-shell singlets calculated using unrestricted broken-symmetry UDFT methods mix closed-shell and open-shell configurations and are not pure spin states. This is reflected by the $\langle S^2 \rangle$ values that are different from 0 (pure singlet) and 2 (pure triplet).

[6] a) E. R. Davidson, *Int. J. Quantum Chem.* **1998**, *69*, 241–245; b) P. M. Lathi, A. S. Ichimura, J. A. Sanborn, *J. Phys. Chem. A* **2001**, *105*, 251–260; c) E. R. Davidson, A. E. Clark, *Int. J. Quantum Chem*. **2005**, *103*, 1–9.

[7] (a) E. Runge, E. K. U. Gross, *Phys. Rev. Lett.* **1984**, *52*, 997–1000; (b) E. K. U. Gross, W. Kohn, *Adv. Quantum Chem.* **1990**, *21*, p. 255; (c) E. K. U. Gross, C. A. Ullrich, U. J. Gossmann, *Density Functional Theory* (Eds.: E. K. U. Gross, R. M. Driezler), Plenum Press, New York, **1995**, p. 149; (d) M. E. Casida, *Recent Advances in Density Functional Methods, Part I* (Ed.: D. P. Chong), World Scientific, Singapore, **1995**, p. 155.

[8] a) H. H. Heinze, A. Görling, N. Rösch, *J. Chem. Phys.* **2000**, *113*, 2088-2099; b) M. Dierksen, S. Grimme, *J. Phys. Chem A* **2004**, *108*, 10225-10237: c) T. M. Halasinski, J. L. Weisman, R. Ruiterkamp, T. J. Lee, F. Salama, M. Head-Gordon, *J. Phys. Chem. A*, **2003**, *107*, 3660-3669.

[9] Y. Gao, C.-G. Liu, Y.-S. Jiang, *J. Phys. Chem A* **200**2, *106*, 5380-5384.